

$^{197}\text{Au}(\gamma, xn; x = 1 \sim 7)$ Reaction Measurements using Laser-Driven Ultra-Bright Ultra-Fast Bremsstrahlung γ -Ray

D. Wu,^{1,2} J.Y. Zhang,^{1,2} H.Y. Lan,^{1,2} J.X. Liu,^{1,2} J.F. Lv,^{1,2} H.G. Lu,^{1,2} X.Z. Wu,^{1,2} H. Zhang,^{1,2} Y.X. Geng,^{1,2} Y.Y. Zhao,^{1,2} J.Y. Xu,¹ J. Cai,³ J.Q. Yu,³ C. Lin,^{1,2} W.J. Ma,^{1,2} H.R. Wang,⁴ F.L. Liu,⁴ C.Y. He,⁴ B. Guo,⁴ G.Q. Zhang,⁵ N.Y. Wang,⁴ Y.G. Ma,⁶ and X.Q. Yan^{1,2,*}

¹State Key Laboratory of Nuclear Physics and Technology,

School of Physics, CAPT, Peking University, Beijing 100871, China

²Beijing Laser Acceleration Innovation Center, Beijing 101407, China

³School of Physics and Electronics, Hunan University, Changsha 410012, China

⁴Department of Nuclear Physics, China Institute of Atomic Energy, Beijing 102413, China

⁵Shanghai Advanced Research Institute, Chinese Academy of Sciences, Shanghai 201210, China

⁶Key Laboratory of Nuclear Physics and Ion-beam Application (MOE),
Institute of Modern Physics, Fudan University, Shanghai 200433, China

(Dated: September 29, 2022)

We present a new method for the measurements of photonuclear reaction flux-weighted average cross sections and isomeric yield ratios using laser-driven ultra-bright ultra-fast bremsstrahlung γ -ray, especially for photonuclear reactions with short half-life times. A 200 TW laser was used to generate stable near-monoenergetic electron beams via laser wakefield acceleration. The flux-weighted average cross sections and isomeric ratios of $^{197}\text{Au}(\gamma, xn; x = 1 \sim 7)$ reactions were analyzed through activation measurements. The results showed good agreements with previous works and were compared with TALYS 1.9 calculations. The $^{197}\text{Au}(\gamma, 7n)^{190}\text{Au}$ reaction cross sections were first achieved. This method offered a unique way of gaining insight into photonuclear reaction researches with short half-life times, which extremely lack experimental data.

Photonuclear reaction cross sections and their isomeric yield ratios are very important in the field of nuclear structures, nuclear reaction mechanisms, and nuclear astrophysics [1–3]. The isomeric yield ratio of a nuclear reaction depends on the projectile particles and the spins of both target and daughter nuclei, which is used as a good test for nuclear structure theories and nuclear reaction models [1, 2, 4, 5]. In nuclear astrophysics, there are 30-35 proton-rich nuclei (p -nuclei) which can not be produced by neutron-capture processes (s -process and r -process) [6–8]. For those nuclei, a lot of processes, known as p -processes, were put forward to explain the p -nucleus production mechanism [7, 9, 10], which contain a series of photonuclear reactions such as (γ, n) , (γ, p) , and (γ, α) reactions [11]. The experimental measurements of those reactions are very important for nuclear synthesis and stellar models [11]. But there are very few studies for cross sections of photonuclear reactions with half-life times of several seconds or less. To explore such reactions, ultra-bright ultra-fast γ -ray sources are required.

The laser electron accelerations [12–18] have attracted significant interest in nuclear physics such as photonuclear studies [19, 20], photon fission [20–22] and photon activation analysis [23]. The laser-driven bremsstrahlung γ -ray source, generated by laser wakefield accelerated (LWFA) electrons, can provide a stable ultra-bright (up to $10^{22\sim 24}$ s⁻¹), ultra-fast (tens of fs), and energy adjustable (keV to hundreds of MeV) photon beam [24–28], which is suitable for photonuclear reaction cross section and isomeric yield ratio measurements. The intensities of laser-driven γ -ray are several orders of magnitude

stronger than other γ -ray sources such as laser Compton scattering (LCS) [29–31] or electron linac bremsstrahlung [32], it is more favorable for the reaction measurements with very short half-lives. In addition, the in-beam background radiation for laser-driven nuclear reactions is highly related to the laser pulse, the duration only last in a nanosecond level, which can provide a very low background environment for online activation measurements and significantly improve the signal-background ratio.

Au material is widely used in photonuclear experiments due to its single nature isotope, high cross sections, and suitable half-life times of the daughter nuclei. The $^{197}\text{Au}(\gamma, xn; x = 1 \sim 3)$ reactions [32–40] and the $^{197}\text{Au}(\gamma, n)^{196m,g}\text{Au}$ isomeric yield ratios [32, 41–48] were measured with different methods, which were often used as high energy γ -ray monitors and applied in experimental method verification. ^{196}Au has two isomeric states: $^{196m1}\text{Au}$ and $^{196m2}\text{Au}$. $^{196m1}\text{Au}$ has a half-life time of 8.1 s and has no available experimental cross section data now. $^{196m2}\text{Au}$ has a half-life time of 9.6h, which can be built up to sufficient intensities. Therefore, the isomeric yield ratios of $^{197}\text{Au}(\gamma, n)^{196m,g}\text{Au}$ reaction is always given by $^{196m2}\text{Au}/^{196m1+g}\text{Au}$. Recently, the $^{197}\text{Au}(\gamma, xn; x = 1\sim 6)$ reaction were measured using an electron linac [32]. The results were compared with previous experiments and theoretical calculations of TALYS 1.6 [49] and TENDL-2014 [50]. The measured cross sections of $^{197}\text{Au}(\gamma, 2n)^{195}\text{Au}$ reaction had a difference of 40% at maximum compared with theoretical values while other data matched very well, it can be presumed that the TALYS 1.6 code could not describe the

$^{197}\text{Au}(\gamma, 2n)^{195}\text{Au}$ reaction very well.

For the first time, the $^{197}\text{Au}(\gamma, xn; x=1\sim 7)$ reaction flux-weighted average cross sections and the $^{197}\text{Au}(\gamma, n)^{196m,g}\text{Au}$ isomeric yield ratios were measured using laser-driven bremsstrahlung γ -ray. The $^{197}\text{Au}(\gamma, 7n)^{190}\text{Au}$ reaction flux-weighted average cross sections were first determined. New theoretical values were calculated and compared with previous experimental results. This new method sheds some light on photonuclear reaction studies with short half-life times. It is expected to fill the experimental data gap of many nuclear reactions.

The experiments were performed at the 200 TW laser facility in Compact Laser Plasma Accelerator (CLAPA) Laboratory, Peking University, which can deliver 4 J, 30 fs, 5Hz laser pulses in the center wavelength of 800 nm. The schematic layout of the experimental setup is shown in Fig. 1. The laser beam was focused to $21 \times 23 \mu\text{m}$ full width at half maximum. The effective energy on target was about 1.8 J with a laser intensity of about $1.5 \times 10^{19} \text{ W}\cdot\text{cm}^{-2}$. The high energy electrons are generated by focusing the laser with a focal length of 100 cm on the leading edge of a $4 \times 1 \text{ mm}$ rectangular supersonic nozzle along the longer direction. The gas jet can provide a supersonic expansion made up of 0.5% Nitrogen and 99.5% Helium mixture gas in vacuum with a maximum air pressure of 45 bar. Electrons are accelerated in LWFA with a monoenergetic spectrum [51]. The maximum electron energies can be adjusted in the range of 60 MeV to 250 MeV with the air pressure of 42 to 27 bar, respectively. The electron energy spectra are analyzed by a 0.8 T magnetic spectrometer 100 cm away from the gas jet, fluorescent screens and CCD cameras are used to record electron signals.

Electron parameters were analyzed before the irradiation experiment. Gas pressures at 33, 36 and 39 bar were used in this work. 100 continuous shoots were recorded at each air pressure for electron parameter analysis, the electron energy stabilities were 91% to 95%, the divergence angle was about 4.3 mrad, the direction stability was better than 5.2 mrad, and the averaged center energies were 135 ± 20 , 103 ± 14 and $78 \pm 10 \text{ MeV}$, respectively, the energy uncertainties were given by the full width at half maximum. The electron charges were $300 \sim 600 \text{ pC}$ measured with a Turbo Integrating Current Transformer (Turbo-ICT) [52] out of a $60 \mu\text{m}$ Be window, which is used to seal the vacuum. An Al foil of $40 \mu\text{m}$ was put before the Be window to reflect the rest of the laser light.

A Ta (99.9%) disk with a size of $2 \times 2 \text{ cm}$ and a thickness of 2 mm, placed at 5 cm before the front surface of magnetic spectrometer, was used as a bremsstrahlung converter. A laminated target made of 1mm ^{197}Au (99.99%), 1 mm ^{27}Al (99.99%), and 1 mm ^{nat}Cu (99.99%) was used for activation analysis in this experiment, all targets had a size of $2 \times 2 \text{ cm}$. The $^{65}\text{Cu}(\gamma, n)^{64}\text{Cu}$ reaction (threshold energy at 9.91 MeV)

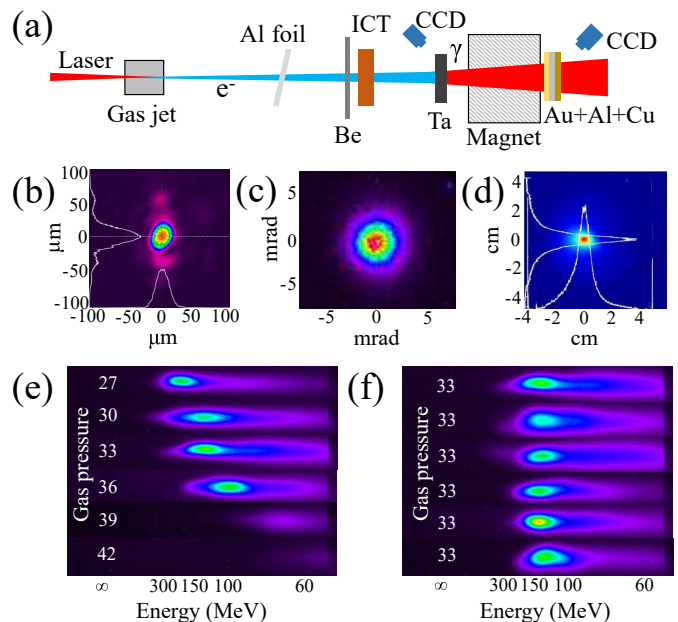


FIG. 1. (a) Schematic layout of experimental setup. (b) Focal laser spot. (c) Electron beam at the front surface of magnetic spectrometer. (d) Electron beam size of 10 continuous shoots at gas pressure of 33 bar measured with a Radiochromic Film (RCF). (e) Electron maximum energies of 60 MeV to 250 MeV at gas pressure of 42 to 27 bar, respectively. (f) Energy stability measured at the back surface of magnetic spectrometer at gas pressure of 33 bar.

and $^{27}\text{Al}(\gamma, 2pn)^{24}\text{Na}$ reaction (threshold energy at 31.45 MeV) were used as γ -ray flux monitors. The repetition frequency was set at 0.25 Hz to keep the vacuum at acceptable levels and the irradiation time was 1 h for each electron energy.

Two HPGe detectors and a LaBr₃ detector were used to measure activation signals 10 min after the irradiation, all detectors were shielded in Pb brick. The detector efficiencies were calibrated with a ^{152}Eu source and a ^{60}Co source, and finally determined by GEANT4 simulations [53, 54]. A typical activation spectrum of the Au target is shown in Fig. 2, the $^{197}\text{Au}(\gamma, xn; x=1\sim 7)$ reactions and $^{197}\text{Au}(\gamma, n)^{196m,2}\text{Au}$ reaction are clearly distinguished.

To obtain the flux-weighted average cross sections of $^{197}\text{Au}(\gamma, xn; x=1\sim 7)$ reactions, effective γ -ray intensity for each electron energy must be determined. The bremsstrahlung γ -ray spectra for each target were calculated by GEANT4 simulation using the averaged electron energy spectra of the 100 continuous shoots before irradiation experiments. The flux-weighted average cross sections of $^{65}\text{Cu}(\gamma, n)^{64}\text{Cu}$ reaction and $^{27}\text{Al}(\gamma, 2pn)^{24}\text{Na}$ reaction were calculated to examine the γ -ray intensities. Experimental flux-weighted average cross sections of $^{197}\text{Au}(\gamma, xn; x=1\sim 7)$ reactions were shown in Tab. I, Fig. 3 and Fig. 4, isomeric ratios of $^{197}\text{Au}(\gamma, n)^{196m,g}\text{Au}$ reaction were also shown in Fig. 4. The statistical errors in this experiment range from 0.74% to 4.5% for

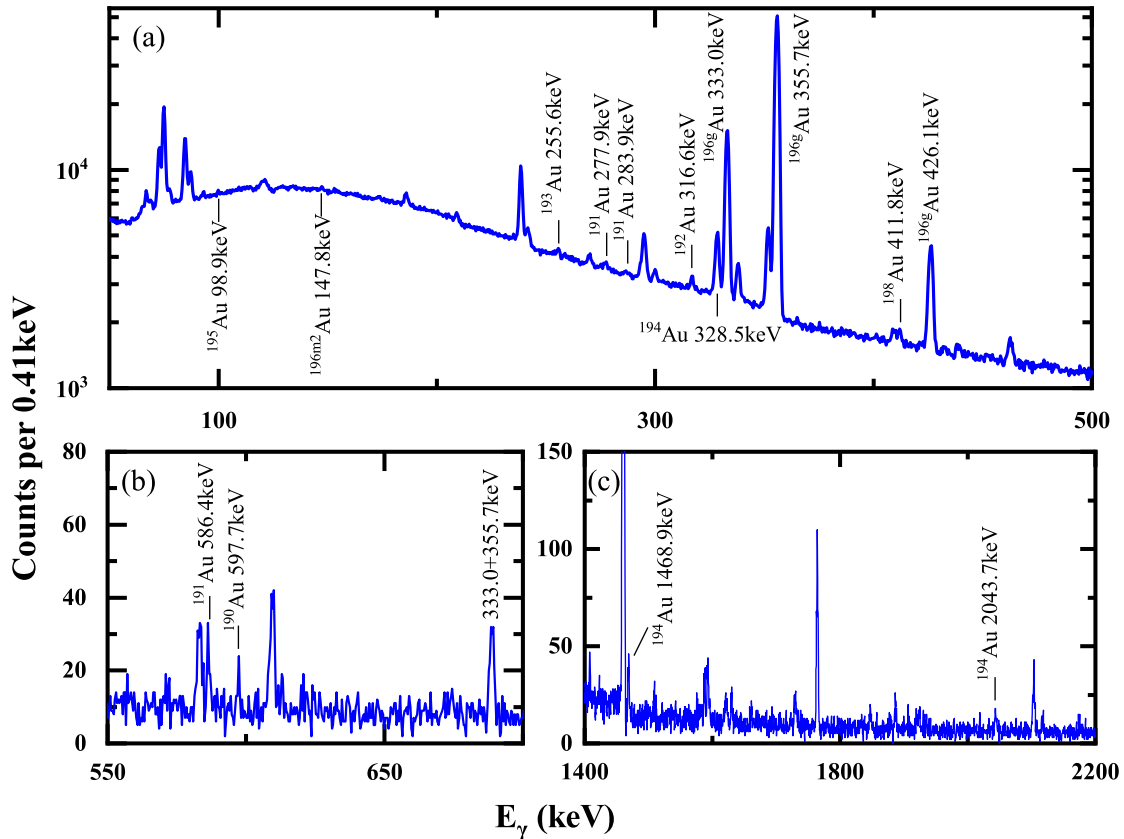


FIG. 2. A typical spectrum of Au target at gas pressure of 36 bar. (a) and (c) were the same spectrum with a long measuring time while (b) has a short measuring time to show the decay of ^{190}Au with a half-life time of 42.8 min. The energies and branch ratios of decay γ -ray were taken from NuDat 3.0 [55].

different decay γ -ray, and the systematic errors include the instabilities of each electron energy, the γ -ray spectra calculation, the calibration of detection efficiency, and the correction of activation target.

Theoretical values of flux-weighted average cross sections and isomeric ratio for the photonuclear reactions of ^{197}Au were calculated by Geant 4 simulation using the data from TENDL-2019 library [56] based on TALYS 1.9 code [57, 58]. As shown in Fig. 3 and Fig. 4, our experimental results matched with previous works and most theoretical values except the $^{197}\text{Au}(\gamma, 2n)^{195}\text{Au}$ reaction. Theoretical values given by TALYS 1.9 are apparently higher than our experiment results by about 37% at maximum, TALYS 1.9 code still can not describe the $^{197}\text{Au}(\gamma, 2n)^{195}\text{Au}$ reaction very well. And for the $^{197}\text{Au}(\gamma, 7n)^{190}\text{Au}$ reaction flux-weighted average cross

sections, first analyzed in this Letter, theoretical values are slightly lower than experiment results. Meanwhile, the $^{197}\text{Au}(\gamma, n)^{196m,g}\text{Au}$ isomeric ratios match well with previous works and theoretical values. The nuclear structure and nuclear reaction mechanisms of ^{197}Au were well restrained by previous works, but for most nuclei, more experimental data are still needed.

In this Letter, we present a new method for the studies of photonuclear reactions using laser-driven γ -ray, which has an ultra-brightness of $10^{22\sim 23} \text{ s}^{-1}$ ($10^{8\sim 9}$ per shoot) and an ultra-short duration of tens fs. This new method offered a unique way of gaining insight into photonuclear reaction cross sections, especially for those reactions with short half-life times which barely had experimental data. The $^{197}\text{Au}(\gamma, xn; x=1\sim 7)$ reactions were measured and compared with previous experimental works and TALYS

TABLE I. The experimental flux-weighted average cross sections of $^{197}\text{Au}(\gamma, xn; x=1\sim 7)$ reactions determined by this work and theoretical values calculated by TALYS 1.9.

Reaction	Center energy of electrons MeV	Experimental cross section mb	TALYS 1.9 ^a mb
$^{197}\text{Au}(\gamma, n)^{196g+m1}\text{Au}$	78 ± 10	95.6 ± 9.9	92.6
	103 ± 14	90.2 ± 9.7	87.1
	135 ± 20	79.5 ± 8.9	76.5
$^{197}\text{Au}(\gamma, n)^{m2}\text{Au}$	78 ± 10	0.0549 ± 0.0063	0.0512
	103 ± 14	0.0538 ± 0.0072	0.0487
	135 ± 20	0.0492 ± 0.0070	0.0461
$^{197}\text{Au}(\gamma, 2n)^{195}\text{Au}$	78 ± 10	25.0 ± 3.9	31.5
	103 ± 14	21.7 ± 3.6	27.5
	135 ± 20	17.9 ± 3.0	24.6
$^{197}\text{Au}(\gamma, 3n)^{194}\text{Au}$	78 ± 10	6.23 ± 0.72	6.2
	103 ± 14	5.35 ± 0.64	5.33
	135 ± 20	5.01 ± 0.59	4.72
$^{197}\text{Au}(\gamma, 4n)^{193}\text{Au}$	78 ± 10	4.92 ± 0.56	4.75
	103 ± 14	4.21 ± 0.48	4.03
	135 ± 20	3.62 ± 0.42	3.51
$^{197}\text{Au}(\gamma, 5n)^{192}\text{Au}$	78 ± 10	3.42 ± 0.40	3.08
	103 ± 14	2.79 ± 0.35	2.53
	135 ± 20	2.36 ± 0.33	2.17
$^{197}\text{Au}(\gamma, 6n)^{191}\text{Au}$	78 ± 10	3.02 ± 0.38	2.81
	103 ± 14	2.45 ± 0.33	2.25
	135 ± 20	1.92 ± 0.25	1.88
$^{197}\text{Au}(\gamma, 7n)^{190}\text{Au}$	78 ± 10	1.81 ± 0.30	1.81
	103 ± 14	1.78 ± 0.27	1.57
	135 ± 20	1.44 ± 0.23	1.24

^a The theoretical values were calculated using a monoenergetic electron beam with the energies of 78, 103 and 135 MeV.

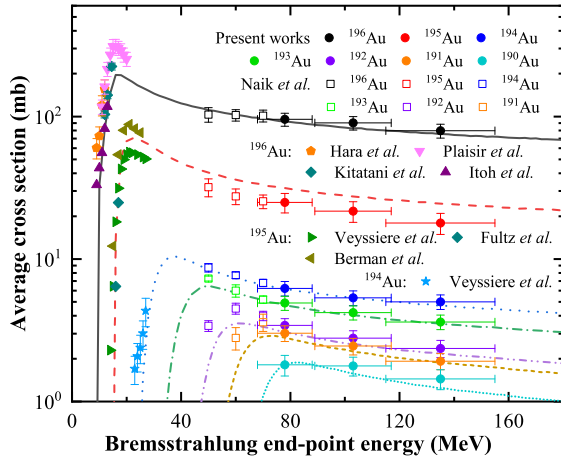


FIG. 3. Experimental results of $^{197}\text{Au}(\gamma, xn; x=1\sim 7)$ reaction flux-weighted average cross sections, compared with previous works [32–40] and TALYS 1.9 calculations (Lines are the flux-weighted average cross sections of $^{197}\text{Au}(\gamma, n)^{196}\text{Au}$ to $^{197}\text{Au}(\gamma, 7n)^{190}\text{Au}$ reaction from the top to the bottom). The bremsstrahlung end-point energies of our experimental cross sections were given as the averaged center electron energies.

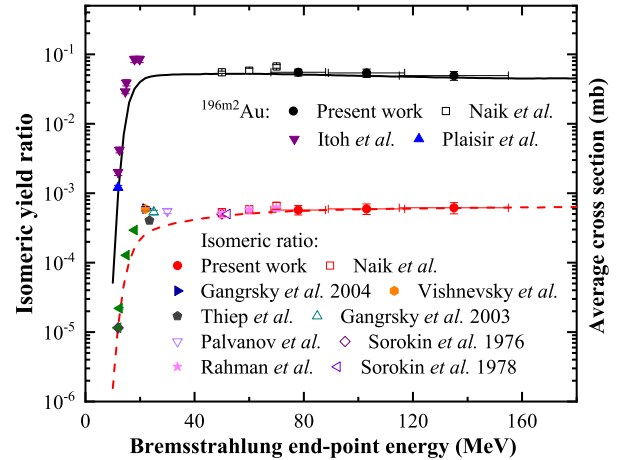


FIG. 4. Experimental results of $^{197}\text{Au}(\gamma, n)^{196m2}\text{Au}$ reaction flux-weighted average cross sections and $^{197}\text{Au}(\gamma, n)^{196m,g}\text{Au}$ isomeric ratios, compared with previous works [32, 39, 41–48] and TALYS 1.9 calculations (Solid line: the $^{197}\text{Au}(\gamma, n)^{196m2}\text{Au}$ reaction flux-weighted average cross sections, dashed line: $^{197}\text{Au}(\gamma, n)^{196m,g}\text{Au}$ reaction isomeric ratios). The bremsstrahlung end-point energies of our experimental cross sections and isomeric ratios were given as the averaged center electron energies.

1.9 calculations, which proved this new method to be accurate. The $^{197}\text{Au}(\gamma, 7n)^{190}\text{Au}$ reaction flux-weighted average cross sections were first measured in this work. The results can be used as monitors in similar experiments.

The authors thank the staff of the 200 TW laser of CLAPA laboratory for the smooth operation of the machine. We thank Professor Wenqing Shen, Professor Baozhen Zhao, and Professor Chong Lv for their helpful comments and suggestions. This work was supported by the National Natural Science Foundation of China (Grants No. 11921006, 12125509), Beijing Outstanding Young Scientists Program, the National Grand Instrument Project (No. 2019YFF01014400), and the Open Foundation of Key Laboratory of High Power Laser and Physics, Chinese Academy of Sciences (No. SGKF202104).

* x.yan@pku.edu.cn

- [1] R. Vandenbosch and J. R. Huizenga, *Phys. Rev.* **120**, 1313 (1960).
- [2] J. R. Huizenga and R. Vandenbosch, *Phys. Rev.* **120**, 1305 (1960).
- [3] M. Blann, *Annu. Rev. Nucl. Sci.* **25**, 123 (1975).
- [4] N. Tsoneva, C. Stoyanov, Y. P. Gangrsky, V. Y. Ponomarev, N. P. Balabanov, and A. P. Tonchev, *Phys. Rev. C* **61**, 044303 (2000).
- [5] D. Kolev and J. Ernest, *Phys. G: Nucl. Part. Phys.* **24**, 589 (1998).
- [6] E. M. Burbidge, G. R. Burbidge, W. A. Fowler, and F. Hoyle, *Rev. Mod. Phys.* **29**, 547 (1957).
- [7] M. Arnould and S. Goriely, *Phys. Rep.* **384**, 1 (2003).
- [8] M. Arnould, S. Goriely, and K. Takahashi, *Phys. Rep.* **450**, 97 (2007).
- [9] A. Sauerwein, M. Elvers, J. Endres, J. Hasper, A. Hennig, L. Netterdon, and A. Zilges, *Prog. Part. Nucl. Phys.* **66**, 363 (2011).
- [10] T. Rauscher, N. Dauphas, I. Dillmann, C. Fröhlich, Z. Fülöp, and G. Gyürky, *Rep. Prog. Phys.* **76**, 066201 (2013).
- [11] W. Rapp, J. Görres1, M. Wiescher, H. Schatz, and F. Käppeler, *Astrophys. J.* **653**, 474 (2006).
- [12] T. Tajima and J. M. Dawson, *Phys. Rev. Lett.* **43**, 267 (1979).
- [13] A. Modena, Z. Najmudin, A. E. Dangor, C. E. Clayton, K. A. Marsh, C. Joshi, V. Malka, C. B. Darrow, C. Danson, D. Neely, and F. N. Walsh, *Nature* **377**, 606 (1995).
- [14] J. Faure, Y. Glinec, A. Pukhov, S. Kiselev, S. Gordienko, E. Lefebvre, J.-P. Rousseau, F. Burgy, and V. Malka, *Nature* **431**, 541 (2004).
- [15] S. Mangles, C. Murphy, Z. Najmudin, A. Thomas, J. Collier, A. Dangor, E. J. Divall, P. S. Foster, J. G. Gallacher, C. J. Hooker, D. A. Jaroszynski, A. J. Langley, W. B. Mori, P. A. Norreys, F. S. Tsung, R. Viskup, B. R. Walton, and K. Krushelnick, *Nature* **431**, 535 (2006).
- [16] C. G. R. Geddes, C. S. Toth, J. V. Tilborg, E. Esarey, C. B. Schroeder, D. Bruhwiler, C. Nieter, J. Cary, and W. P. Leemans, *Nature* **431**, 539 (2004).
- [17] A. Pukhov and J. M. ter Vehn, *Appl. Phys. B* **74**, 355 (2002).
- [18] W. Lu, C. Huang, M. Zhou, W. B. Mori, and T. Katsouleas, *Phys. Rev. Lett.* **96**, 165002 (2006).
- [19] K. Ledingham, I. Spencer, T. McCanny, R. Singhal, M. Santala, E. Clark, I. Watts, F. N. Beg, M. Zepf, K. Krushelnick, M. Tatarakis, A. E. Dangor, P. A. Norreys, R. Allott, D. Neely, R. J. Clark, A. C. Machacek, J. S. Wark, A. J. Cresswell, D. C. W. Sanderson, and J. Magill, *Phys. Rev. Lett.* **84**, 899 (2000).
- [20] P. Boller, A. Zylstra, J. Burggraf, G. Henry, L. Bernstein, C. Brabetz, J. Glorius, J. Hellmund, J. Hornung, Y. Litvinov, P. Neumayer, O. Rosmej, V. Bagnoud, T. Kuehl, D. H. Schneider, and J. Jeet, *Nuclear Excitation and Fission Studies with Short Pulsed Laser-Driven High Energy Gamma Rays*, Technical Report (Lawrence Livermore National Lab., Livermore, CA, United States, 2021).
- [21] K. Boyer, T. Luk, and C. Rhodes, *Phys. Rev. Lett.* **60**, 557 (1988).
- [22] T. Cowan, A. Hunt, T. Phillips, S. Wilks, M. Perry, C. Brown, W. Fountain, S. Hatchett, J. Johnson, M. H. Key, T. Parnell, D. M. Pennington, R. A. Snavely, and Y. Takahashi, *Phys. Rev. Lett.* **84**, 903 (2000).
- [23] F. Mirani, D. Calzolari, A. Formenti, and M. Passoni, *Commun. Phys.* **4**, 185 (2021).
- [24] A. Giulietti, N. Bourgeois, T. Ceccotti, X. Davoine, S. Dobosz, P. D'Oliveira, M. Galimberti, J. Galy, A. Gamucci, D. Giulietti, L. A. Gizzi, D. J. Hamilton, E. Lefebvre, L. Labate, J. R. Marquès, P. Monot, H. Popescu, F. Réau, G. Sarri, P. Tomassini, and P. Martin, *Phys. Rev. Lett.* **101**, 105002 (2008).
- [25] J. Ferri, S. Corde, A. Döpp, A. Lifschitz, A. Doche, C. Thauray, K. T. Phuoc, B. Mahieu, I. A. Andriyash, V. Malka, , and X. Davoine, *Phys. Rev. Lett.* **120**, 254802 (2018).
- [26] S. Li, B. F. Shen, J. C. Xu, T. J. Xu, Y. Yu, J. F. Li, X. M. Lu, C. Wang, X. L. Wang, X. Y. Liang, Y. X. Leng, R. X. Li, and Z. Z. Xu, *Phys. Plasmas* **24**, 093104 (2017).
- [27] A. Döpp, E. Guillaume, C. Thauray, A. Lifschitz, F. Sylla, J.-P. Goddet, A. Tafzi, V. Malka, A. Rousse, and K. T. Phuoc, *Nucl. Instrum. Methods Phys. Res. A* **930**, 515 (2016).
- [28] M. Günther, O. Rosmej, P. Tavana, M. Gyrzymov, A. Skobliakov, A. Kantsyrev, S. Zähter, N. G. Borisenko, A. Pukhov, and N. E. Andreev, *Nat. Commun.* **13**, 170 (2022).
- [29] H. R. Weller, M. W. Ahmed, H. Y. Gao, W. Tornow, Y. K. Wu, M. Gai, and R. Miskimen, *Prog. Part. Nucl. Phys.* **62**, 257 (2009).
- [30] K. Horikawa, S. Miyamoto, S. Amano, and T. Mochizuki, *Nucl. Instrum. Methods Phys. Res. A* **618**, 1 (2010).
- [31] H. W. Wang, G. T. Fan, L. X. Liu, H. H. Xu, W. Q. Shen, Y. G. Ma, H. Utsunomiya, L. L. Song, X. G. Cao, Z. R. Hao, K. J. Chen, S. Jin, Y. X. Yang, X. R. Hu, X. X. Li, and P. Kuang, *Nucl. Sci. Tech.* **33**, 87 (2022).
- [32] H. Naik, G. Kim, K. Kim, M. Zaman, A. Goswami, M. W. Lee, S. C. Yang, Y. O. Lee, S. G. Shin, and M. H. Cho, *Nucl. Phys. A* **948**, 28 (2016).
- [33] S. Fultz, R. Bramblett, J. Caldwell, and N. Kerr, *Phys. Rev.* **127**, 1273 (1962).
- [34] A. Veyssiere, H. Bell, R. Bergere, P. Carlos, and A. Lepretre, *Nucl. Phys. A* **159**, 561 (1970).
- [35] B. Berman, R. Pywell, S. Dietrich, M. Thompson, K. Mc-

- neill, and J. Jury, Phys. Rev. C **36**, 1286 (1987).
- [36] K. Hara, H. Harada, F. Kitatani, S. Goko, S. Hohara, T. Kaihori, A. Makinaga, H. Utsunomiya, H. Toyokawa, and K. Yamada, J. Nucl. Sci. Technol. **44**, 938 (2007).
- [37] F. Kitatani, H. Harada, S. Goko, H. Utsunomiya, H. Akimune, T. Kaihori, H. Toyokawa, and K. Yamada, J. Nucl. Sci. Technol. **47**, 367 (2010).
- [38] F. Kitatani, H. Harada, S. Goko, H. Utsunomiya, H. Akimune, H. Toyokawa, and K. Yamada, J. Nucl. Sci. Technol. **48**, 1017 (2011).
- [39] O. Itoh, H. Utsunomiya, H. Akimune, T. Kondo, M. Kamata, T. Yamagata, H. Toyokawa, H. Harada, F. Kitatani, S. Goko, C. Nair, and Y. W. Lui, J. Nucl. Sci. Technol. **48**, 834 (2011).
- [40] C. Plaisir, F. Hannachi, F. Gobet, M. Tarisien, M. M. Aléonard, V. Méot, G. Gosselin, P. Morel, and B. Morillon, Eur. Phys. J. A **48**, 68 (2012).
- [41] A. A. Sorokin and V. N. Ponomarev, in: Report of the 26th Conference on Nuclear Spectroscopy and Structure of Atomic Nuclei, Nauka, Leningrad , p.449 (1976).
- [42] A. A. Sorokin, in: Report of the 28th Conference on Nuclear Spectroscopy and Structure of Atomic Nuclei, Alma-Ata , p.258 (1978).
- [43] S. R. Palvanov and O. Razhabov, At. Energ. **87**, 75 (1999).
- [44] Y. P. Gangrsky, N. N. Kolesnikov, V. G. Lukashik, and L. M. Melnikova, Bull. Russ. Acad. Sci. Phys. **67**, 1772 (2003).
- [45] Y. P. Gangrsky, N. N. Kolesnikov, V. G. Lukashik, and L. M. Melnikova, Phys. At. Nucl. **67**, 1227 (2004).
- [46] T. D. Thiep, T. T. An, N. T. Vinh, P. V. Cuong, A. G. Belov, O. D. Maslov, and T. T. T. My, Phys. Part. Nucl. Lett. **3**, 223 (2006).
- [47] I. Vishnevsky, V. Zheltonozhsky, I. Kadenko, E. Kulich, V. Plyujko, and N. Strilchuk, Bull. Russ. Acad. Sci., Phys. **72**, 1569 (2008).
- [48] M. S. Rahman, K. S. Kim, M. W. Lee, G. N. Kim, Y. D. Oh, H. S. Lee, M. H. Cho, I. S. Ko, W. Namkung, V. D. Nguyen, D. K. Pham, T. T. Kim, and T. I. Ro, J. Radioanal. Nucl. Chem. **283**, 519 (2004).
- [49] A. Koning, S. Hilaire, and M. Duijvestijn, *Nuclear Excitation and Fission Studies with Short Pulsed Laser-Driven High Energy Gamma Rays*, TALYS-1.6, A nuclear reaction program, NRG-1755 NG Petten (Lawrence Livermore National Lab., The Netherlands, 2008).
- [50] A. Koning and D. Rochman, Nucl. Data Sheets **113**, 2841 (2012).
- [51] A. Pukhov, S. Gordienko, S. Kiselev, and I. Kostyukov, Plasma Phys. Control. Fusion **46**, B179 (2004).
- [52] K. Nakamura, D. E. Mittelberger, A. J. Gonsalves, J. Daniels, H. S. Mao, F. Stulle, J. Bergoz, and W. P. Lee-mans, Plasma Phys. Control. Fusion **58**, 034010 (2016).
- [53] S. Agostinelli, J. Allison, K. A. Amako, J. Apostolakis, H. Araujo, P. Arce, *et al.*, Geant4—a simulation toolkit, Nucl. Instrum. Methods A **506**, 250 (2003).
- [54] J. Allison, K. Amako, J. Apostolakis, H. Araujo, P. Dubois, M. Asai, and A. Heikkinen, IEEE Tran. Nucl. Sci. **53**, 270 (2006).
- [55] NuDat 3.0 (National Nuclear Data Center, Brookhaven National Laboratory, 2022).
- [56] A. Koning, D. Rochman, J. Sublet, N. Dzysiuk, M. Fleming, and S. van der Marck, Nucl. Data Sheets **155**, 1 (2019).
- [57] A. Koning and D. Rochman, Nucl. Data Sheets **133**, 2841 (2012).
- [58] E. Alhassan, D. Rochman, A. Vasiliev, M. Hursin, A. J. Koning, and H. Ferroukhi, Nucl. Sci. Tech. **33**, 105 (2022).